ORIGINAL RESEARCH PAPER

Evaluation of thermal and antimicrobial behavior of Montmorillonite nanoclay modified with 2-Mercaptobenzothiazole

Milad Edraki [1], Davood Zaarei [1]*

[1] *Polymer Department, Technical Faculty, South Tehran Branch, Islamic Azad University, Tehran, Iran*

ABSTRACT

Thermal and antimicrobial properties of hybrid synthesized compounds were evaluated in the present study. Hybrid structures were synthesized via two main organic and inorganic components, namely: 2-Mercaptobenzothiazole (MBT) and sodium Montmorillonite clay (Na+-MMT). The synthesis process took place in a direct reaction, intercalation; and the resulting material was characterized. Results of scanning electron microscope (SEM), Energy dispersive X-ray spectroscopy (EDS), transmission electron microscope (TEM), and small-angle X-ray scattering (SAXS) and Fourier transform infrared spectroscopy (FTIR) confirmed MBT penetration of particles into the inner space of the clay layers and interaction between the two organic and inorganic phases. Also, thermal properties of the resulting compounds were evaluated by thermo gravimetric analysis (TGA) and differential thermalgravimetric (DTG). It was found that while MBT sample had relatively low degradation temperature (about 250°C), the MBT-modified clay compound showed superior thermal stability, and in high temperatures, less weight loss as compared to MBT. Antimicrobial properties of the hybrid nano compound against five types of bacteria, two types of fungus and one type of yeast were examined using well diffusion agar method and minimum inhibitory concentration (MIC). The diameter of inhibition zone was measured and their antimicrobial potential was compared with two common antibiotics: gentamicin and rifampin. The concentration of about 1000 μg/mL of MBT-MMT showed antibacterial performance equal to 250 μg/mL of rifampin. Also, 1000 μg/mL of this material was required to inhibit the growth of important bacteria.

Keywords: *Clay, layered silicate, Hybrid compounds, Thermal stability, Antimicrobial properties.*
© 2018 Published by Journal of Nanoanalysis.

INTRODUCTION

Montmorillonite (MMT) falls into the clay and plate-like clay category [1]. Plates of this material are made up of two tetrahedral sheets and one octahedral sheet, attached to each other [2]. Tetrahedral sheets, including hexagonal rings, are made up of silicon-oxygen units; octahedral sheets are composed of silicon-aluminum units, in which some of the aluminum or silicon ions are replaced by ions with less capacity such as magnesium [3]. Therefore, layers of this substance have negative electric charge and this negative charge balances with positive charges of sodium or calcium cations

* Corresponding Author Email: *d_zarei@azad.ac.ir*

between layers. MMT layers have one-nanometer thickness and length equal to hundred nanometers with parallel arrangement, and form bulks using physical forces. The distance between the layers is displayed with d_{001} symbol [1-4].

MMT is a hydrophilic material, but by exchanging cations between its layers with a variety of organic amines, it can become a hydrophobic material known as organic clay. The layered structure of organic clays with nanometer dimensions has provided grounds for this material to be used in polymer nanocomposite coatings [3].

The presence of MMT particles in polymer matrix, due to the nature of clay including high surface area, low permeability and slow-down in the production of volatile compounds, has led to the formation of carbon charcoal layer on the surface of the polymer which can act as protection for the substrate material and also because of surface gas absorption by MMT platelets, resulting in increased heat resistance [5]. On the other hand, the plate structure of MMT prolongs the flow direction of corrosive species, inhibits the absorption of aggressive ions in the surface and increases corrosion resistance and barrier properties [2,6].

2-Mercaptobenzothiazole (MBT) organic material has a wide range of applications including as a corrosion inhibitor for protection of various metal surfaces [7-9]. Its mechanism of action is as follows: operates through adsorption process and create a hydrophobic protective layer on the metal surface, which poses a barrier to the dissolution of the metal in the electrolyte (as both anodic and cathodic inhibitor) [8]. On the other hand, MBT organic materials contain many sulfur groups in their structure, therefore acting as antifungal and antibacterial compounds [10-12].

Destruction of organic materials inside the polymer matrix against thermal factors results in limiting application in many cases such as high temperature coatings, insulations, etc. Therefore, MBT should be encapsulated in high-temperature conditions, as a result, its thermal evaluation is highly important.

Kaya et al. [13] synthesized a hybrid nanopigment based on bentonite clay nano particles and Rhodamine B (Rh B) dye. Using a TGA test, a conclusion was drawn in that, hybrid-synthesized nano-pigments revealed a good thermal stability with 25% of weight reduction till 750°C, while Rh B lost 96% of its weight at the same temperature range.

Sternik et al. [14] synthesized a hybrid nanopigment based on sodium bentonite (Na$^+$-bentonite) and Basic Red 1 (BR1) dye. They also studied the thermal behavior of synthesized pigment by using TGA. Ultimately, they concluded that the noted nanopigment lost 21% of its weight till 900°C, while BR1 dye lost 100% of its weight at the same temperature range, and was fully destroyed. The main reason for thermal stability of clay-based nanopigment is that the clay layers prevent thermal loading on the molecular structure of the dyes.

In this study, hybrid inorganic-organic compounds, consisting of Na$^+$-MMT and MBT were synthesized. Intercalation of inorganic clay with organic MBT was studied using SAXS, FTIR, SEM/EDS and TEM test methods. Moreover, thermal behavior of synthesized compositions was investigated employing TGA and DTG methods. At the end, Well Diffusion Agar and MIC tests were used to evaluate the antimicrobial properties of these hybrid nanocompounds.

EXPERIMENTAL

Materials
2-Mercaptobenzothiazole (MBT), deionized water and ethyl alcohol were supplied by Merck Company (Germany). The inorganic clay used in this study was sodium Montmorillonite (Na$^+$-MMT). This material was purchased from Rockwood Company (USA).

Instruments
For the objectives of the study, X-ray diffraction (XRD) studies on the Na$^+$-MMT and hybrid synthesized compounds (MBT-MMT) were carried out employing a Bruker SAXS D8 Small angle Xray diffractometer (Cu-Kα radiation, 40 kV, 35 mA). The data were collected for angles 2θ from 2 to 15°. The basal spacing d_{001} was calculated from the basal reflections using the Bragg's law. Eq.1 is as follows:

$$(n\lambda = 2d\sin\theta) \qquad (1)$$

FTIR spectra of Na$^+$-MMT, MBT and MBT-MMT were run on a VERTEX 70 Bruker company (Germany) by KBr pressed disk method. The spectra were collected for each measurement over the spectral range of 400 to 4000 cm^{-1} with a resolution of 4 cm^{-1}.

The morphology of MBT-MMT nano-particles

was examined by Scanning Electron Microscope (SEM) model LEO 1455 VP and Zeiss EM900 Transmission Electron Microscope (TEM) with the accelerating voltage of 80 KV. For SEM test, the mentioned samples were covered with a thin layer of gold, and prepared through sputtering method. For TEM test, samples were prepared by depositing a diluted suspension of nanoparticles on a carbon copper grid and allowing them to dry before the analysis. Identification of the chemical elements of MBT-MMT was done by energy dispersive X-ray spectroscopy (EDS) analyzer and the used software was ZAF.

Thermal analysis of the Na^+-MMT, MBT,and MBT-MMT was conducted using a Perkin Elmer Instrument. The test was carried out under nitrogen atmosphere with temperature range and heating rate of 30-600^{0}C and 10^{0}C/min, respectively.

Synthesis process

In order to synthesize the compounds, 5 g of Na^+-MMT was dispersed in 350 ml of ethyl alcohol and stirred with magnetic stirrer for one hour. This process resulted in swelling of the clay platelets and release of exchangeable cations from inter-layer space in solvent environment. In another vessel, 1.24 g of MBT was dissolved in 100 ml of ethyl alcohol by manual mixing, and the resulting mixture was then transferred to the first vessel. This solution was stirred with magnetic stirrer for 24 h at room temperature in order to insert MBT molecules into the interlayer space of clay particles. After that, the solution was allowed to be in a stasis position for 48 h to precipitate. For separation of synthesized modified clay compounds, a centrifuge device (model EBA21, Hettich Company), with 6000 r/min, was used for 15 min In the last phase, sediments were washed with deionized water and remained in vacuum oven for 24 h so that a dry and light powder can be produced.

Antimicrobial test

The microorganisms used in this research are:

Two types of Gram-positive bacteria including *Staphylococcus epidermidis* (ATCC 12228) and *Staphylococcus aureus* (ATCC 29737), three types of Gram-negative bacteria including *Salmonella Paratyphi-A serotype* (ATCC 5702), *Escherichia coli* (ATCC 10536) and *Sheigella dysenteriae* (PTCC 1188), one type of yeast *Candida albicans* (ATCC 10231), and two types of fungus including *Aspergillus niger* (ATCC 16404) and *Aspergillus*

brasiliensis (PTCC 5011). The stages for performing the antimicrobial tests are as follows:

First stage: Well diffusion

The fresh culture was prepared from the mentioned bacteria (Gram-positive and negative). A suspension of 0.5 McFarland was prepared from the bacteria and was lawn cultured on Muller-Hinton Agar culture medium. Wells with diameter of 6 mm were created in the environment and 10 µL of 30 mg/mL was poured into the wells from the compound of interest. The plates were incubated for 24 h at 37°C. Thereafter, the plates were examined in terms of zone of inhibition diameter and the results were reported.

Second stage: Minimum inhibitory concentration (MIC)

Seven dilutions were prepared from MBT-MMT compounds: 2000, 1000, 500, 250, 125, 62.50 and 31.25 µg/mL were the concentrations of the relevant compound. Next, 96-well microplates were used, where the microplates had 12 weight-well rows.

In each vertical row from top to bottom, seven dilutions prepared as 100 µL were poured. For example, 5 µL bacteria plus 95 µL of the medium Tryptic Soy Broth (TSB) together with 100 µL from the first dilution.

The third stage: MIC of fungi

The seven dilutions which were used in the previous stage including the minimum inhibitory concentration of the bacteria were mixed with Sabouraud Dextrose (SD) medium and the prepared plate was inoculated unto the fungi of interest as follows. After the incubation time at 30°C, the plates were examined in terms of growth of fungi and the last plate in which no fungal growth was observed was considered as the fungal MIC.

RESULTS AND DISCUSSION

Small angle X-ray diffraction analysis

Figure 1 illustrates XRD curves for sodium montmorillonite clay (Na^+-MMT) and hybrid synthesized compound (MBT-MMT). As shown in the figure, maximum peak of Na^+-MMT emission is about $2\theta = 7.4°$. Based on the Braggs law, d-spacing is about. $d = 11.37 A°$. X-ray diffraction curve of MBT-MMT depicts that the emission peak is about 4.9°; therefore, the d-spacing (d_{001}) was about 18.00 $A°$. This reveals that 2-mercaptobenzothiazole (MBT) molecules have penetrated into the

interlayer space (galleries) of nanoclay. Therefore, d-spacing increased up to about 6.63 $A°$. Diffraction characteristics of sodium montmorillonite nanoclay and hybrid synthesized compounds are shown in table 1.
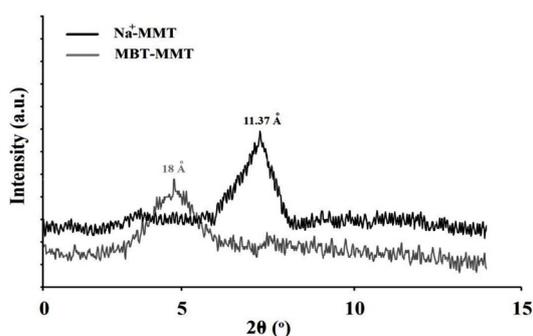

Fig. 1. XRD patterns of Na+-MMT clay and MBT-MMT.

Table 1. Interlayer distances of Na+ - MMT and MBT-MMT system obtained by XRD

Samples	$2\theta°$	$d_{001} [A°]$	$\Delta cl [A°]$
Na+ - MMT	7.4	11.37	6.63
MBT- MMT	4.9	18.00	

Fourier transform infrared spectroscopy

Figure 2 clearly shows FTIR spectrum for a) Na+-MMT, b) MBT and c) MBT-MMT. As shown in the figure, for Na+-MMT , 465.82 cm-1 peak demonstrates Si-O bending vibration (in plane) group; 525.08 cm-1 peak illustrates Si-O-Al vibration and MgO group; 621.95cm-1 peak indicates Mg-O-Si or Fe-O-Si groups; 799.53 cm-1 peak shows AlMgOH vibration group; 917.48 cm-1 peak shows Al$_2$OH bending group; 1044.04 cm-1 peak reveals Si-O stretching vibration (in plane) group; 1638.27, 1702.36 and 3448 cm-1 peaks depict OH bending and stretching vibration groups, and finally, 3632.67 cm-1 peak represents OH stretching group [13].

In MBT, 421.57 cm-1 peak is indicative of S-C=S bending group; 568.86 and 599.23 cm-1 peaks reveal C-S group; 661.03, 1908.47, 1954.78, 2355.17 and 2454.93 cm-1 peaks depict N=C=S group; 7482.51 and 853.73 cm-1 peaks indicate aromatic C-H group; 1031.13, 1076.17 and 1131.62 cm-1 peaks display N-C=S and C=S group; 1242.09, 1279.63, 1421.02, 1454.02 and 1493 cm-1 peaks show C-N-H and C-C stretching group; 1315 cm-1 peak demonstrate CH$_3$ group; 1591.11 cm-1 peak reveals C=C stretching and CS$_2$ groups; 2508.16, 2574.92, 2671.02, 2739.98, 2836.12 and 2891 cm-1 peaks illustrate S-H group; 2960.90, 3038.43 and 3073.88 cm-1 peaks demonstrate asymmetric CH group and finally, 3112.30 cm-1 peak represents asymmetric NH stretching group [15,16]. However, in synthesized MBT-MMT substance, 423.96 cm-1 peak shows S-C=S bending group; 436.69 and 523.53 cm-1 peaks illustrate Si-O bending vibration in clay plane and Si-O-Al vibration, respectively; 663.99, 1953.23 and 2359.44 cm-1 peaks display N=C=S group; 566.07 and 601.51 cm-1 peaks depict C-S group; 748.31 cm-1 indicates aromatic C-H group; 1032.08, 1075.29 and 1127.21 cm-1 peaks reveal N-C=S and C=S groups; 1242.74, 1280.34, 1422.43, 1455.33 and 1494.58 peaks represent C-N-H and C-C stretching groups; 1316.97 cm-1 peak shows CH$_3$ group; 1592.26 cm-1 peak demonstrates C=C stretching and CS$_2$ groups; 1640.93 and 3434.80 cm-1 peaks indicate OH bending and stretching vibration groups; 2505.56, 2737.74, 2834.71 and 2890.55 cm-1 peaks depict S-H group and finally 2959.60, 3037.37 and 3073.18 cm-1 peaks reveal asymmetric CH stretching group. It can be concluded that there is interaction between functional groups of MMT and MBT, confirming the construction of new structures apart from clay and MBT. The type of this interaction is hydrogen bond, since S-H group of hydrogen in MBT forms a hydrogen bond with the OH group inside the structure of Na+-MMT and the relevant peak can be observed in the frequency of 3434 cm−1.

Scanning electron microscope and Energy dispersive X-ray spectroscopy

Figure 3 depicts the SEM images of Na+-MMT and MMT-MBT with different magnifications. As shown in Figure 3, the appearance of raw MMT after modification with MBT is different. This is due to the processing used for preparation of MMT-MBT. High shear mixing processes broke the clay structure, and appearance was influenced by the amplitude of these mechanical forces. With attention on dissolving the MBT particles in ethanol and very small dimensions of this organic molecule, distinguishing the

penetrated and interacted molecular size MBT particles into the clay, by SEM, was impossible and it was only the structure of synthesized clays that appeared.

Additionally, EDS analysis confirmed the results of XRD and FTIR test results.
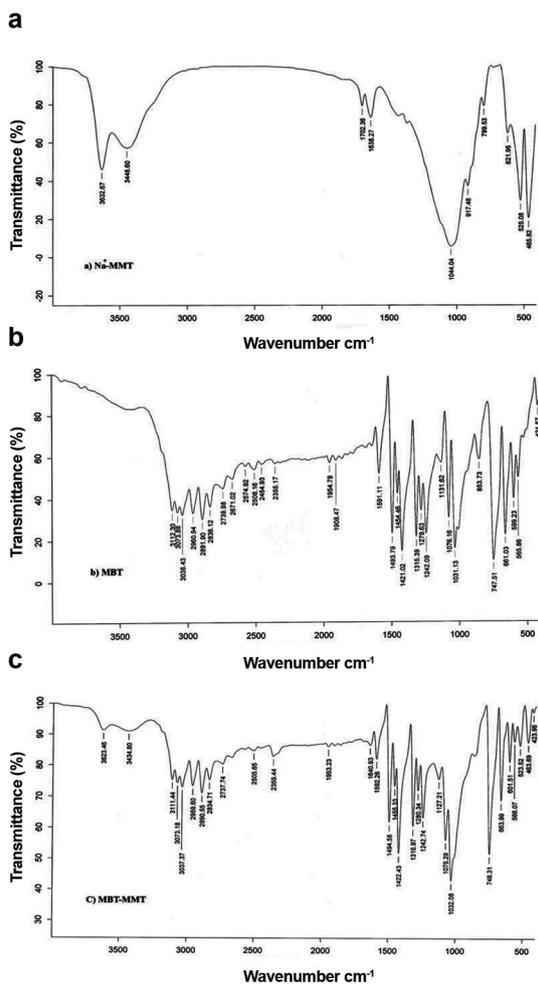
a

b

c

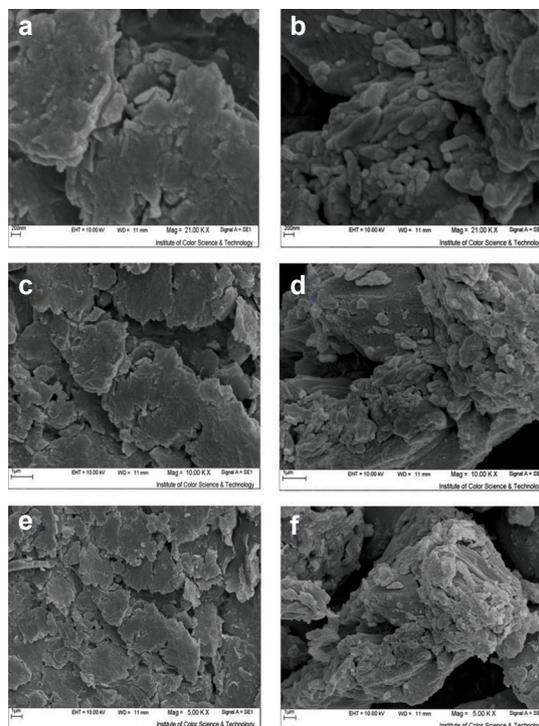Fig. 2. FTIR spectra of (a) Na$^+$-MMT, (b) MBT and (c) MBT-MMT.

Fig. 3. SEM analysis of Na$^+$-MMT sample with magnification of 21X (a), 10X (b), 5X (c), and MBT-MMT sample with magnification of 21X (d),10X (e) and 5X (f).

Figure 4 indicates the results of elemental analysis for MBT-MMT sample using EDS. As shown in Figure 4, the most constituent component of hybrid synthesized compound is MMT mineral phase (about 67.6 %), which includes Si: 28.2, Al: 10.2, O: 20.1, Fe: 4.24 and Mg: 4.86, the rest of which comprises MBT organic phase (about 32.4 %), including C: 20.3, N: 4.3 and S: 7.8, which reveals the interaction between the two phases and insertion of MBT molecules in Na$^+$-MMT inter-layer space.

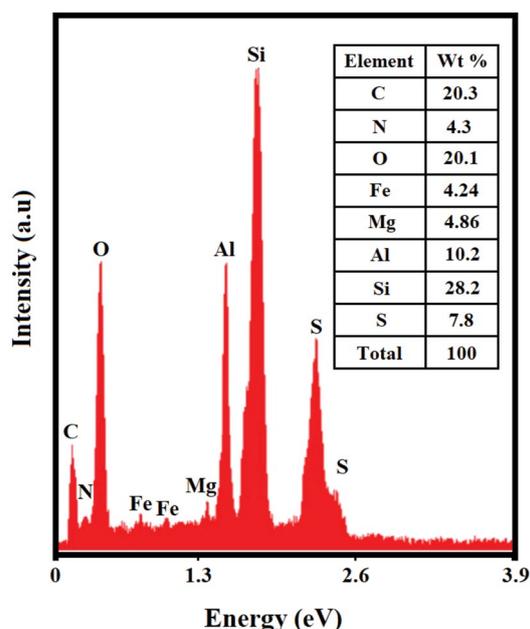| Element	Wt %
C	20.3
N	4.3
O	20.1
Fe	4.24
Mg	4.86
Al	10.2
Si	28.2
S	7.8
Total	100

Fig. 4. Elemental analysis of the MBT-MMT using EDS.

Transmission electron microscope of synthesized compounds

Figure 5a and b show the images of TEM relating to Na$^+$-MMT and MBT-MMT with the same magnifications. Black and white lines in the image below represent the silicate layers of clay minerals. TEM images clearly confirm the interlayer structure of MBT-MMT layer in which the penetration of molecules of MBT organic material increased the interlayer space (gallery) of Na$^+$-MMT. With all these, Na$^+$-MMT retained its structure, which means it is intercalated (interlayered) but not laminated (exfoliated). In the case of lamination, the distance between the plates became more than 100 angstroms. On the other hand, mixing technique was effective for the separation of accumulated MBT-MMT compounds. TEM results are in line with x-ray diffraction and SEM results, and demonstrate that the formation of hybrid compounds occurs with a nanometer planar structure.

Thermal analysis of synthesized compounds

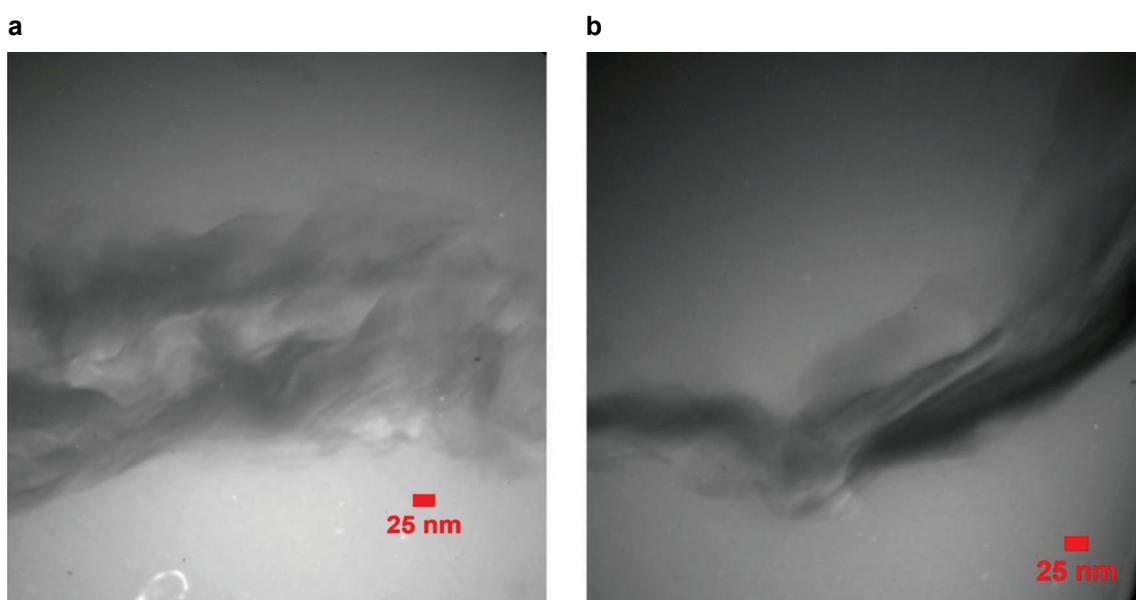Figure 6 reveals thermo gravimetric analysis (TGA) curves of Na$^+$-MMT, MBT and MBT-MMT samples.

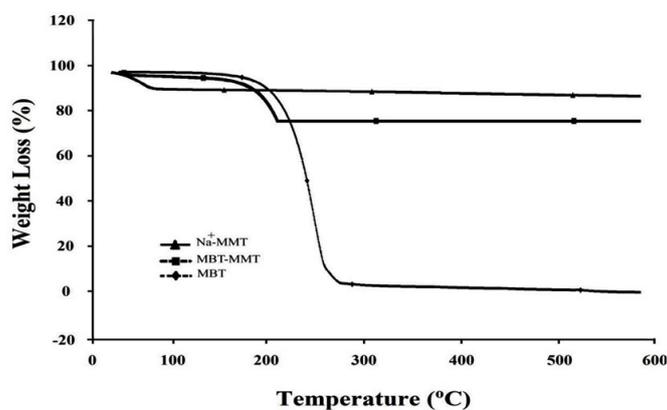Fig. 5. TEM images 85000X magnification related to a) Na$^+$-MMT, b) MBT-MMT.

Fig. 6. TGA curves for Na$^+$-MMT, MBT and MBT-MMT.

As shown in Figure 6, Na$^+$-MMT sample indicated approximately 8.3% weight loss in the temperature range of 30- 200°C in the first stage, which is due to dehydration inside the interlayer space of clay. In the temperature range of 200-600°C, it displayed a 2.02% weight loss. It might be due to the dehydroxylation of inorganic clay [17-23]. Thermal degradation of MBT molecules occurs in one step. TGA curve of this compound had a gentle slope to a temperature of less than 204°C and partially showed a weight loss of 3.5%, which is adsorbed due to the physical water loss and water bonds within the MBT molecule (moisture loss). Overall loss of MBT occurs in the range of 205-516°C. The molecule experienced a 96.5% weight loss in this temperature range, which can be caused by thermal degradation of the resulted functional groups of N=C=S and C-S [15, 24-27].

Regarding MMT-MBT substance obtained by the interaction of Na$^+$-MMT and MBT, there was a 7.2% weight loss in the temperature range of 30-200°C in the first stage, triggered by dehydration inside the interlayer space of clay. In the next stage and in the temperature range of 200-400°C, there was a 15.5% weight loss, which was due to the thermal degradation of organic MBT molecules adsorbed on the outer platelets of clay. In the next stage and in the temperature range of 400-600°C, a one-percent weight loss indicating dehydroxylation of inorganic clay was shown. Based on the data obtained from the EDS analysis conducted on MBT-MMT and comparing these data with the results of TGA analysis, it can be concluded that about 16.9 wt% of 32.4 wt% of MBT material has been inserted into the clay inter-layer space and the rest (about) 15.5 wt% has been adsorbed in clay outer surface and was thereby degraded. Figure 6 also shows that the degradation temperature of MBT in hybrid synthesized compound was about 235°C.

Figure 7 represents differential thermal gravimetric (DTG) for Na$^+$-MMT, MBT and MBT-MMT samples. As shown in this figure, for Na$^+$-MMT sample, differential weight loss peaks are in the temperatures of 80, 150 and 570°C, and for MBT substance, differential weight loss peaks are in temperatures of 170, 250, 285 and 550°C. For MBT-MMT sample, peak temperatures of 170, 235, 260 and 520°C showed weight loss.

Complete information on thermal analysis of the mentioned compounds is represented in Table 2.

As shown in table 2, peak temperature for dehydration (about 80°C) was omitted in MMT-MBT, so it can be concluded that the hydrophilic nature of MMT, after interaction with MBT, has changed to a hydrophobic one. Also, due to presence of organic species in MMT-MBT, the final DTG peak temperature reduced from 570 to 520°C, resulting in interaction between species in clay and organic MBT.

Evaluation of the antimicrobial properties of MBT-MMT hybrid nanocompound

In table 3, given the sterilized conditions, the performance of the eight types of microorganism in the presence of two common antibiotics: gentamicin and rifampin as control, are provided.

As shown in table 3, at MIC point, the performance of these two bacterial inhibitory compounds ranged between 250 and 500 μg/mL, which changes given the type of bacteria. It is noteworthy that in spite of function within the bacterial inhibitory range, these two compounds have no function against fungi and yeasts and developed no inhibition.

Table 2. Thermal analysis of Na$^+$-MMT, MBT and MBT-MMT

Samples	Weight loss [%] at Temperature [°C]			Total weight loss [%]	DTG Peak temperature [°C]
	30-200	200-400	400-600		
Na$^+$ - MMT	8.3	0.9	1.12	10.32	80,150,570
MBT	3.5	96	0.5	100	170,250,285,550
MBT-MMT	7.2	15.5	1	23.7	170, 235,260, 520
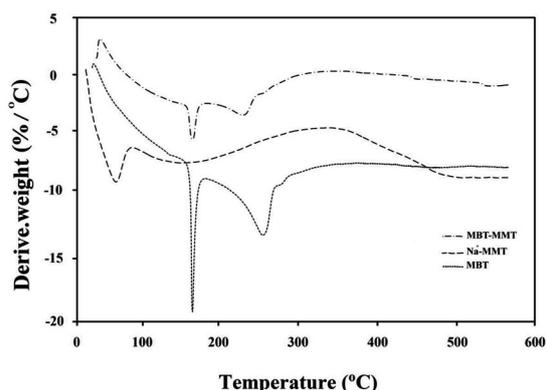
Fig. 7. DTG curves for of Na⁺-MMT, MBT and MBT-MMT.

the seven prepared concentrations. The results suggest that unlike gentamicin and rifampin, which had no fungicidal function, this compound had this property at very low concentrations of about 62.5 µg/mL. The notable point is that the inhibitory and fungicidal points are at the same concentration, and after this concentration and with its elevation, the fungicidal function is completed. In this regard, the minimum inhibitory concentration on the yeast ATCC10231 is about 1000 µg/mL, which corresponds to the point of the minimum bactericidal concentration (MBC). The results show that for important bacteria, 1000 µg/mL are required to inhibit the growth and function, where in industrial uses, application of this compound (MBT-MMT) should be considered in the coatings.

Table 4 provides the minimum inhibitory and bactericidal concentrations for MBT-MMT across

Table 3. Performance of the common antibiotics in terms of minimum inhibitory concentration under laboratory conditions, on the bacteria, fungi and yeast samples [28]

Antibiotic	Concentration (µg/ml)	gram-positive bacteria			gram-negative bacteria		yeast	Fungus	
		(ATCC 29737)	(ATCC 12228)	(PTCC 1188)	(ATCC 10536)	(ATCC 5702)	(ATCC 10231)	(ATCC 16404)	(PTCC 5011)
Rifampin	250	MIC*	MIC	MIC	growth	ineffective	NA**	NA	NA
	500	B.S***	B.S	B.S	MIC	ineffective	NA	NA	NA
	250	growth	growth	growth	growth	growth	NA	NA	NA
Genntamici	500	MIC	MIC	MIC	MIC	MIC	NA	NA	NA

* MIC: minimum inhibitory Concentration.
** NA : No Active.
*** B.S: Bacterio Static.

Table 4. The performance of MBT-MMT in terms of minimum inhibitory and bactericidal concentrations, on different microorganisms

Sample	Concentration (µg/ml)	gram-positive bacteria			gram-negative bacteria		yeast	Fungus	
		(ATCC 29737)	(ATCC 12228)	(PTCC 1188)	(ATCC 10536)	(ATCC 5702)	(ATCC 10231)	(ATCC 16404)	(PTCC 5011)
	31.25	growth	growth	growth	growth	growth	growth	growth	growth
	62.50	growth	growth	growth	growth	growth	growth	MIC=MBC*	MIC=MBC*
	125	growth	growth	growth	growth	growth	growth	_	_
MBT-MMT	250	growth	growth	growth	growth	growth	growth	_	_
	500	growth	MIC	growth	growth	growth	growth	_	_
	1000	MIC	B.S	MIC	MIC	MIC	MIC=MBC	_	_
	2000	MBC>2000	MBC	MBC	MBC	MBC	_	_	_

As shown in table 5, the factor: diameter of inhibition zone suggests the potential of the compound in controlling antibacterial properties. In this regard, the two control compounds: rifampin and gentamicin were examined alongside MBT-MMT. The diameter of inhibition zone for all the samples at MBC or MIC concentrations is provided in the table. As shown, the performance of MBT-MMT is relatively weaker than that of gentamicin, yet it showed better performance and efficiency than rifampin. As rifampin is used as an antibacterial compound in pharmaceuticals, it can be said that the concentration of about 1000 μg/mL of MBT-MMT has a performance equal to 250 μg/mL of rifampin.

Table 5. The diameter of zone of inhibition in terms of mm at MBC or MIC for MBT-MMT, gentamicin and rifampin, in the presence of different microorganisms

Microorganism	Inhibition zone diameter (mm)		
	(MBT-MMT)	(Gentamicin)	(Rifampin)
ATCC 29737	11	21	10
ATCC 12228	28	35	40
PTCC 1188	11	18	8
ATCC 10536	10	21	11
ATCC 5702	15	21	–
ATCC 10231	23	NA	NA
ATCC 16404	29	NA	NA
PTCC 5011	24	NA	NA

CONCLUSION

Results of SAXS obviously showed that due to the penetration of MBT organic molecules into the interlayer space of Na+-MMT, the d-spacing between the clay platelets increased and intercalation took place.

Results of FTIR and EDS analysis depicted that, after interaction of MBT with Na+-MMT, functional groups of MBT have appeared on modified nanoclay structure

Modification of montmorillonite clay by MBT resulted in a different morphology of clay, in comparison with neat particles.

Results of TGA showed that about 23.7% weight loss of MBT-MMT, in the temperature range of 30-600°C, was happened, while MBT organic material showed 100% destruction within the same temperature range. The major reason for thermal stability of synthesized compound (MBT-MMT), as compared to MBT, was the fact that the clay layers acted as a heat shield and inhibited the thermal loading on the molecular structure of MBT.

DTG analysis showed that the peak temperature for dehydration was disappeared in MBT modified clay, and the hydrophilic nature of this material was changed into a hydrophobic one. Also, interaction between species of clay and organic MBT led to lowering the peak temperature of modified clay from 570 to 520 oC.

Excellent fungicidal and anti-yeast properties were observed in MBT modified clay, and this material can be used as an antibacterial compound in pharmaceuticals and coating materials.

CONFLICT OF INTEREST

The authors declare that there is no conflict of interests regarding the publication of this manuscript.

REFERENCE

1. A. A. Azeez, K.Y. Rhee, S. J. Park, and D. Hui, Composites Part B., 45(1), 308 (2013).
2. H.R. Zamanizadeh, M.R. Shishesaz, I. Danaee, and D. Zaarei, Prog. Org. Coat., 78, 256 (2015).
3. M. Edraki, and M. Banimahd Keivani, J. Phys. Theor. Chem. IAU Iran., 10(1), 69 (2013).
4. M. Kotal, and A. K. Bhowmick, Prog. Polym. Sci., 51, 127(2015).
5. D. Xiao, Z. Li, X. Zhao, U. Gohs, U.Wagenknecht, B.Voit, and D. Y.Wang, Appl. Clay Sci., 143, 192 (2017).
6. A.H. Navarchian, M. Joulazadeh, and F. Karimi, Prog. Org. Coat., 77(2), 347 (2014).
7. M. Edraki, and D. Zaarei, Iranian patent 92996 (2017).
8. F. Maia,K. A.Yasakau,J.Carneiro,S.Kallip,J.Tedim,T. Henriques, and M. G. S. Ferreira, Chem. Eng. J., 283, 1108 (2016).
9. A. Rahimi, and S. Amiri, J. Coat. Technol., 12(3), 587 (2015).
10. M. A. Azam, and B. Suresh, Sci. Pharm. 80(4), 789 (2012).
11. M.F. Mahdi, R.F. Al-Smaism, and N.W. Ibrahim, European Journal of Chemistry. , 7(1), 8 (2016).
12. A. Kuznetsova, P.M. Domingues,T. Silva, A. Almeida, M.L. Zheludkevich, J. Tedim, M.G.S. Ferreira, and A. Cunha, J. Appl. Microbiol., 122(5), 1207 (2017).
13. M. Kaya,Y. Onganer, and A. Tabak, J. Phys. Chem. Solids., 78, 95 (2015).
14. D.Sternik,M.Majdan,A.Deryło-Marczewska,G. Żukociński,A.Gładysz-Płaska,V. M.Gun'ko, and S.

V.Mikhalovsky, J. Therm. Anal. Calorim., 103(2), 607 (2011).

15. N.B. Sanches, S.N. Cassu, and R. D. C. L. Dutra, Polímeros., 25(3), 247 (2015).

16. N. AlHokbany, and I. AlJammaz, Open Journal of Inorganic Chemistry. , 1(2), 23 (2011).

17. A. Ghazi, E. Ghasemi, M. Mahdavian, B. Ramezanzadeh, and M. Rostami, Corros. Sci., 94, 207 (2015).

18. V. Marchante Rodríguez, F.M. Martínez-Verdú, M.I. Beltrán Rico, and A. Marcilla Gomis, Pigm Resin Technol., 41(5), 263 (2012).

19. V. Marchante, A. Marcilla,V. Benavente, F.M. Martínez-Verdú, and M.I. Beltran, J. Appl. Polym. Sci., 129(5), 2716 (2013).

20. V. Marchante,V. Benavente,A. Marcilla,F.M. Martínez-Verdú, and M.I. Beltrán, J. Appl. Polym. Sci., 130(4), 2987 (2013).

21. S. Raha, N. Quazi,I. Ivanov, and S. Bhattacharya, Dyes pigm., 93(1), 1512 (2012).

22. M. Edraki, and D. Zaarei, Iranian patent 88184 (2016).

23. M.I. Beltrán,V. Benavente,V. Marchante,H. Dema, and A. Marcilla, Appl. Clay Sci., 97, 43 (2014).

24. A. Samide, P. Rotaru, C. Ionescu,B. Tutunaru,A. Moanţă, and V. Barragan-Montero, J. Therm. Anal. Calorim., 118(2), 651(2014).

25. Y. Li, S. Zhang, Q. Ding, D. Feng, B. Qin, L. Hua, TRIBOL INT. ,114,121(2017).

26. K.V. Yeole,I.P. Agarwal, and S.T. Mhaske, J. Coat. Technol., 13(1), 31(2016).

27. D. Yu, J. Wang, W. Hu, and R. Guo, Mater. Des., 129, 103 (2017).

28. M. Edraki, and D. Zaarei, Asian J. Green Chem., DOI: 10.22631/ajgc.2018.114758.1049, (2018).